inorganics

MDPI

Review

Cell Metabolomics to Guide the Design of Metal-Based Compounds

Veronica Ghini

Department of Chemistry, University of Florence, Via della Lastruccia 3, Sesto Fiorentino, 50019 Florence, Italy; ghini@cerm.unifi.it

Abstract: Despite the increasing interest in the development of novel metal-based compounds for cancer treatment, these molecules are currently poorly characterized in mechanistic terms, due to their multiple macromolecular targets inside the cells. In this review, we show how ^{1}H NMR metabolomics provides a powerful tool to investigate the metabolic perturbations induced by metal-compounds in cells. The chemical identity and concentration of metabolites detected in cell lysates and their respective growth media by NMR can be viewed as a global fingerprint that describes the response to drug treatment. In this framework, the applications of NMR-based metabolomics to study cellular effects induced by the treatment of cells with anticancer metal-based compounds are comprehensively reviewed.

Keywords: metal-based compounds; NMR; metabolomics

check for updates

Citation: Ghini, V. Cell Metabolomics to Guide the Design of Metal-Based Compounds. *Inorganics* **2024**, *12*, 168. https://doi.org/10.3390/inorganics12060168

Academic Editors: Irena Kostova and Luciano Saso

Received: 9 May 2024
Revised: 11 June 2024
Accepted: 13 June 2024
Published: 15 June 2024

1. NMR-Based Cell Metabolomics

Metal-based compounds constitute a variegate family of very promising drugs for cancer treatment [1,2]. Despite the huge interest, their intracellular modes of action and targets remain to be elucidated to a large extent. In fact, the nature of the metal ion, its oxidation state, along with the nature of its ligands, all contribute to the cellular reactivity of the complex, modulating the affinity for different intracellular targets as well as its ability to cross biological membranes. Thus, it is not easy to predict a priori the cellular behavior of these complexes.

In this context, NMR-based metabolomics of cell cultures constitutes an ideal tool to gain information about the cellular modes of action of the different metal complexes in an accessible, manageable, and practical biological setup [3,4]. Metabolomics is a methodology focused on the analysis of all the metabolites (i.e., small molecules with a molecular weight <2 kDa, according to the definition of the Human Metabolome Database [5]) that are present in a biological sample. This technique has the ability to bring to light variations in the levels of intra- and extra-cellular metabolites induced by drug treatments and these changes can be directly related to the up- or down-regulation of specific pathways involved in the drug's modes of action [3,6–9]. This methodological approach also offers the possibility to identify specific markers of tumor responsiveness or development of resistance to anticancer metal complexes.

Among all the NMR active nuclei, ^{1}H is doubtless the most used for metabolomic applications. The overall ^{1}H NMR spectral profile of cells constitutes an untargeted fingerprint of the NMR-detectable portion of their whole metabolome. Each type of cell line is characterized by a typical NMR fingerprint that can be considered as a dynamic mirror of its metabolic profile. The metabolomic fingerprint contains information on the number and relative concentration of the most abundant (>1 μM) metabolites that take part in the main metabolic pathways of the cell, i.e., a pool of 30–40 metabolites including amino acids, nucleotides, sugars, organic acids, etc. It is important to note that with NMR, the only metabolites that are detectable are (i) the metabolites that do not interact with macromolecules present in solution (such as proteins) or (ii) the fractions of the interacting metabolites that are free in solution, in exchange with the bound fractions; the bound fraction is, instead, invisible [10,11].

In Figure 1 the metabolomic fingerprints of the A2780 ovarian cancer cell line, GL261 glioblastoma cell line, and DAOY medulloblastoma cell line are reported as an example.

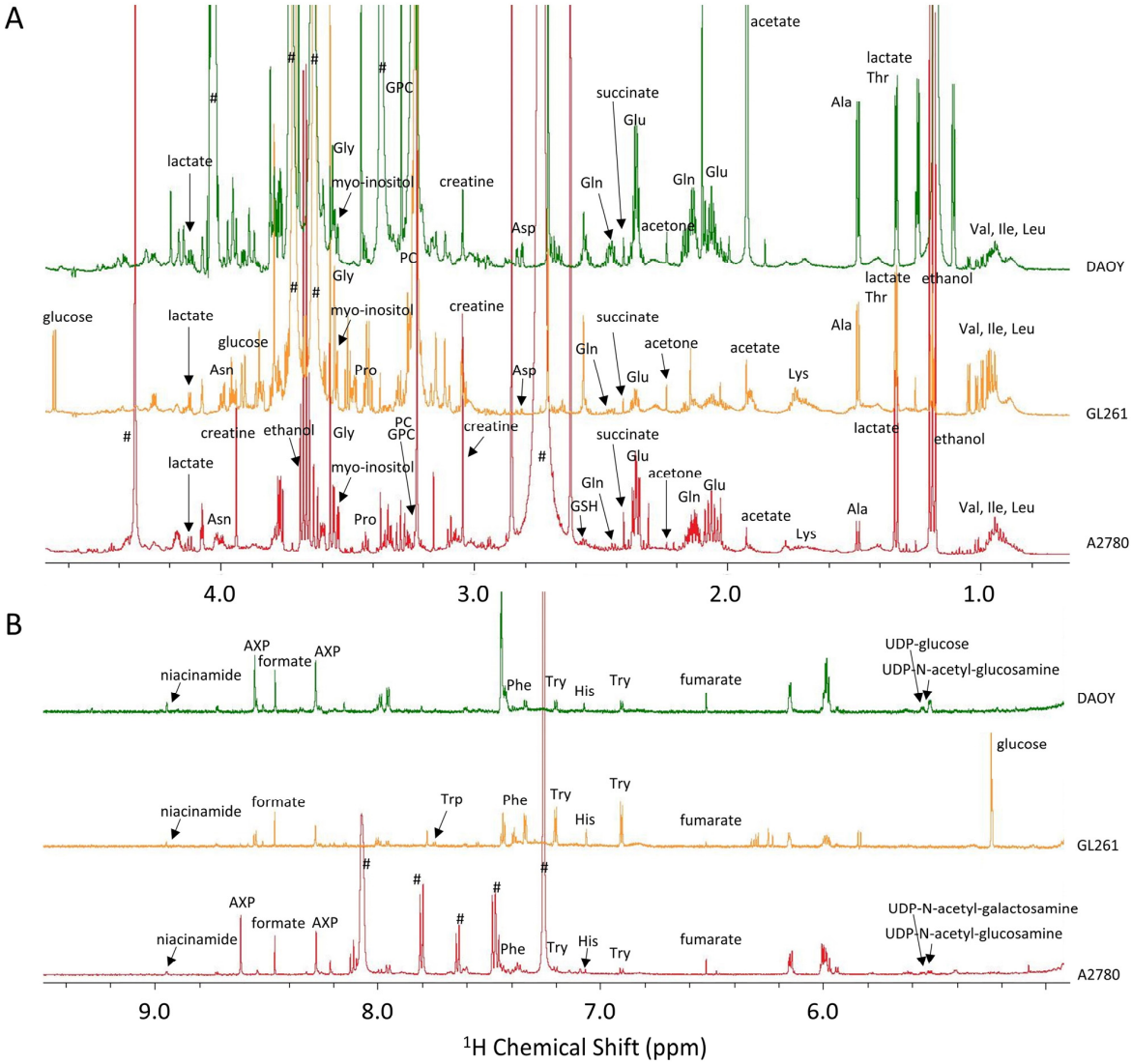

Figure 1. Representative ^{1}H NMR spectra of the endo-metabolome (cell lysates) of A2780 ovarian cancer cells (red trace), GL261 glioblastoma cells (yellow trace), and DAOY medulloblastoma cells (green trace). (**A**) Upfield (1.00–4.50 ppm) and (**B**) downfield (5.00–9.50 ppm) regions. The most abundant metabolites that have been identified in the spectra are indicated; for a graphical reason, for each metabolite only one (or more for a few cases) resonance is reported. Abbreviations: phosphocholine (PC); glycerophosphocholine (GPC); glutathione (GHS); ATD/ADP/AMP (AXP); #: signals arising from protease and phosphatase inhibitor cocktails. The samples have been prepared according to the protocol reported in [3].

Since a substantial fraction of metabolites of the central metabolism are phosphorylated (nucleotides, intermediates of glycolysis, the pentose phosphate pathway, etc.), ^{31}P NMR can be used to expand the coverage of the metabolome but also to monitor lipids (phospholipids, phosphocholines, etc.) [12]. ^{31}P NMR has also proven to be a powerful, non-perturbing probe of membranes whose composition influences their biophysical properties that, in turn, are important for metal-based drug uptake and resistance development [13].

For the analysis of the cell metabolome (endo-metabolome), a fast quench of the cellular metabolism is required to obtain reliable fingerprints. One of the most common quenching methods consists of the use of cold methanol (approx. −40 to −50 °C).

Subsequently, chloroform is added to separate the two phases, i.e., polar and non-polar extracts [6,7,14].

Our lab developed a fast and highly reproducible protocol for the analysis of the endo-metabolome that avoids extraction [3]. The protocol is based on procedures usually adopted in western blot proteomics, where the cells are scraped into phosphate buffer and supplemented with a protease and phosphatase inhibitor cocktail diluted in dimethyl sulfoxide (DMSO) that is used to quench enzymatic reactions and stabilize the cellular metabolism. The cells are then lysed by sonication in ice, centrifuged, and finally the supernatant is recovered for the analysis. This procedure allows the obtainment of cell lysates that are stable on the time scale of the NMR sample acquisition [15]. As a drawback, the components of the cocktail of inhibitors present as free molecules in solution give rise to NMR resonances that may overlap with the NMR signals of the metabolites (see Figure 1).

Additionally, high-resolution magic angle spinning (HR-MAS) NMR offers the possibility of obtaining the metabolomic fingerprint of intact cells, avoiding the step of cell breaking [16]. This allows the analysis of the real-time metabolome of viable cells until degradation processes occur. In Figure 2, the metabolomic fingerprint of intact human endometriotic epithelial 12Z cells is reported as an example. The method has been used in several studies for the characterization of cultured 2D cells [17], and more recently in 3D cultures [18], as they represent in vivo features more accurately than standard 2D systems (see Table 1).

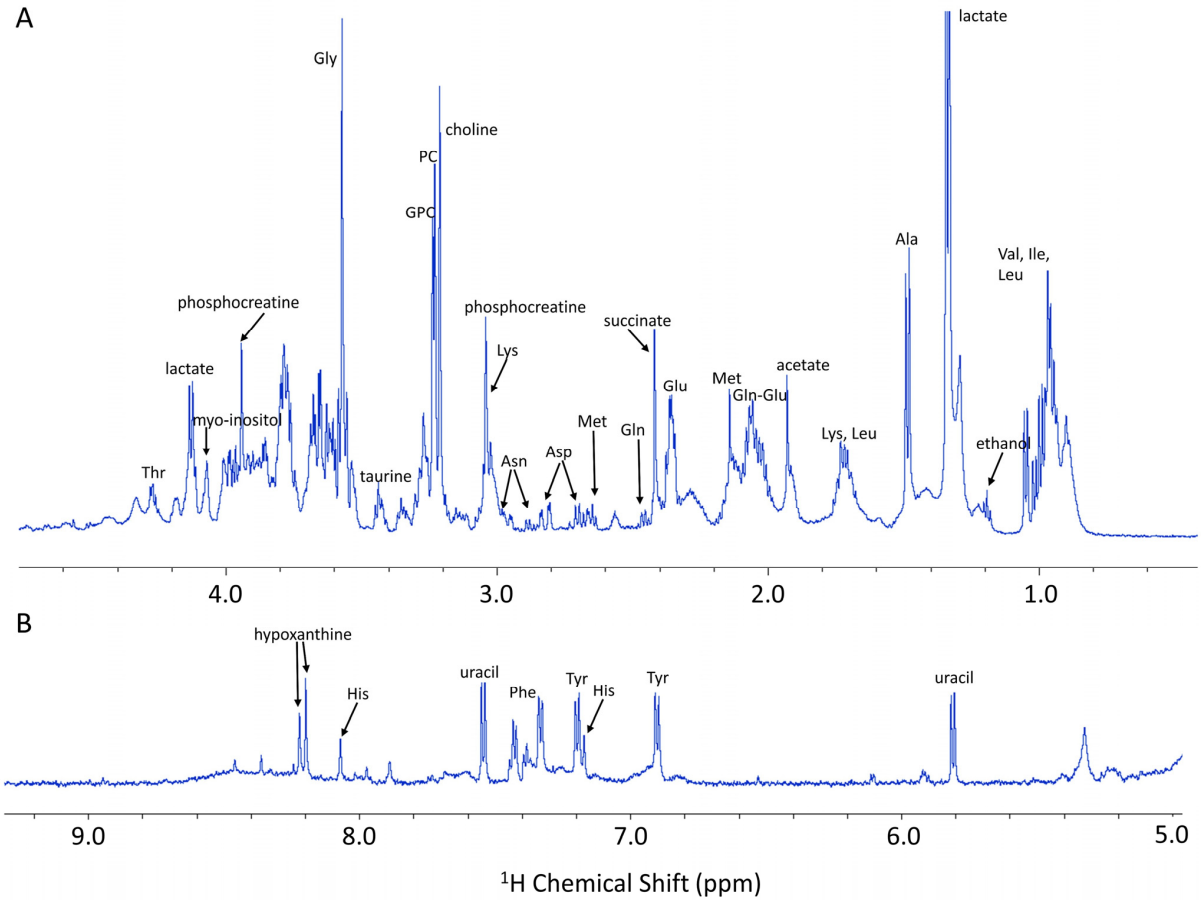

Figure 2. Representative ^{1}H HR-MAS spectrum of intact human endometrial epithelial 12Z cells. (**A**) Upfield (1.00–4.50 ppm) and (**B**) downfield (5.00–9.00 ppm) regions. The most abundant metabolites that have been identified in the spectra are indicated; for a graphical reason, for each metabolite only one (or more for a few cases) resonance is reported. Abbreviations: phosphocholine (PC); glycerophosphocholine (GPC).

Table 1. NMR-based metabolomic studies on the cellular effects of metal-based compounds. In the case of comparisons of different compounds, only the structures of metal compounds are reported. m/c = methanol/chloroform; m/c/w = methanol/chloroform/water.

Ref	Compound(s)	Structure(s)	Cell Line(s)	Type of Experiments	Sample Type(s)	Drug Treatment (Concentration)	Exposure Time
			Platinum				
[19]	Cisplatin	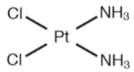	Human liver L02 cells	^{1}H NMR	Cell extracts (m/c/w)	1 nM, 1 μM and 1 mM	24 h
[20]	Cisplatin	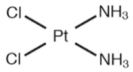	Human lung cancer A549 cells	^{1}H HR-MAS	Cell lysates	IC_{50} at 24 h	12, 18, 24, 36, 48 h
[21]	Cisplatin	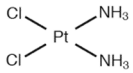	• Human medulloblastoma DAOY cells • Human supratentorial primitive neuroectodermal tumor PFSK-1 cells	• ^{1}H HR-MAS • ^{1}H NMR	• Intact cells • Lipid droplet extracts (m/c)	10 μM	12, 24, 48 h
[22]	Cisplatin	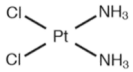	Human osteosarcoma MG-63 cells	^{1}H HR-MAS	Cell lysates	IC_{50} at 24 h (30 μM) and 50 μM	12, 18, 24, 48 h
[23]	Cisplatin	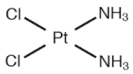	• Rat glioblastoma BT4C cells • Human glioblastoma U87-MG cells • Human medulloblastoma DAOY cells • Human supratentorial primitive neuroectodermal tumor PFSK-1 cells	• ^{1}H HR-MAS • ^{1}H NMR	• Intact cells • Cell extracts (m/c)	10 μM	12, 24, 48 h
[24]	• Cisplatin • Carboplatin • Oxaliplatin	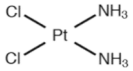 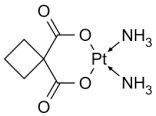 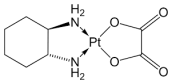	• Human ovarian cancer A2780 cells • Human cisplatin-resistant ovarian cancer A2780cis cells	^{1}H NMR	• Cell lysates • Growth media	IC_{50} at 72 h	24, 48 h

Table 1. *Cont.*

Ref	Compound(s)	Structure(s)	Cell Line(s)	Type of Experiments	Sample Type(s)	Drug Treatment (Concentration)	Exposure Time
[25]	• Cisplatin • Biphenyl nicotinamide compound • Vinblastine	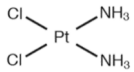	Human breast cancer MCF-7 cells	^{1}H NMR	Cell lysates	IC_{50} time not specified	72 h
[26]	• Cisplatin • Doxorubicin • Methotrexate	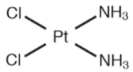	Human osteosarcoma MG-63 cells	^{1}H HR-MAS	Cell lysates	IC_{50} at 24 h	12, 24, 36, 48 h
[27]	• Doxorubicin • Tamoxifen • Cisplatin	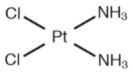	Human breast cancer MDA-MB-231 cells	^{1}H HR-MAS	Intact cells	Not specified	24 h
[28]	• Oxaliplatin • Oxaliplatin • + vitamin C	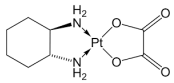	Human hepatocellular carcinoma HCC SMMC-7721 cells	^{1}H NMR	Cell extracts (m/c/w)	50 μM oxaliplatin	48 h
[29]	• [Pt(O,O′-acac)(γacac)(DMS)] • Cisplatin	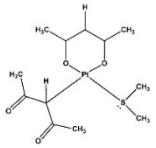 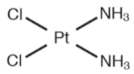	Human cisplatin-resistant ovarian cancer Skov-3 cells	^{1}H NMR	• Cell extracts (m/c/w) • Growth media	IC_{50} at 24 h	6, 12, 24 h

Table 1. *Cont.*

Ref	Compound(s)	Structure(s)	Cell Line(s)	Type of Experiments	Sample Type(s)	Drug Treatment (Concentration)	Exposure Time
[30]	• $[Pt(\eta^1C_2H_4OMe)(DMSO)(phen)]^+$ • Cisplatin	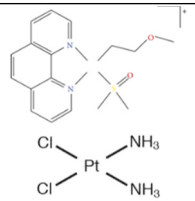	Human neuroblastoma cancer SH-SY5Y cells	^{1}H NMR	• Cell extracts (m/c/w) • Growth media	IC_{50} at 24 h	6, 12, 24 h
Gold							
[31]	Auranofin	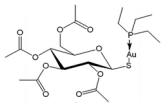	Human ovarian cancer A2780 cells	^{1}H NMR	• Cell lysates • Growth media	IC_{50} at 72 h	3, 6, 12, 24 h
[32]	Auranofin conjugated with the nanocarrier ferritin	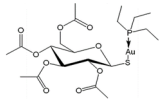	Human ovarian cancer A2780 cells	^{1}H NMR	• Cell lysates • Growth media	IC_{50} at 72 h	24 h
[33]	• Au(NHC)Cl • $[Au(NHC)_2]PF_6$	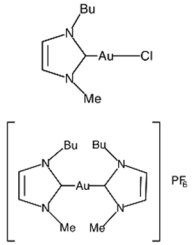	Human ovarian cancer A2780 cells	^{1}H NMR	• Cell lysates • Growth media	IC_{50} at 72 h	6, 12, 24 h
Ruthenium							
[34]	$[(\eta^6\text{-}p\text{-}MeC_6H_4iPr)_2Ru_2(\mu\text{-}S\text{-}p\text{-}C_6H_4tBu)_3]Cl$ (DiRu-1)	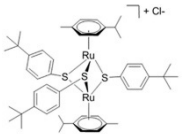	• Human ovarian cancer A2780 cells • Human cisplatin-resistant ovarian cancer A2780cis cells • Human embryotic kidney HEK-293 cells	^{1}H HR-MAS	Cell lysates	IC_{50} time not specified	24 h

Table 1. *Cont.*

Ref	Compound(s)	Structure(s)	Cell Line(s)	Type of Experiments	Sample Type(s)	Drug Treatment (Concentration)	Exposure Time
[35]	(■^{6}-p-cymene) Ru(Cl_2) (PPh_2(p-MeBenzoate) NCH_2CH_2N (pMeBenzoate) (PPh_2)(Cl_2)Ru(■^{6}-p-cymene) (*GA113*)	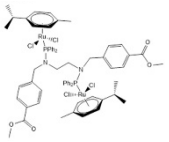	Human melanoma A375 cells	^{1}H NMR	Cell extracts (m/c)	IC_{50} at 24 h	24 h
[17]	[(p-cymene)$_6$Ru$_6$ (tpt)$_2$(dhnq)$_3$]$^{6+}$	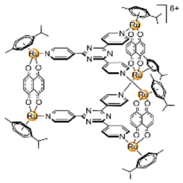	• Human ovarian cancer A2780 cells • Human cisplatin-resistant ovarian cancer A2780cis cells • Human embryotic kidney HEK-293 cells	^{1}H HR-MAS	Intact cells	IC_{50} at 96 h	24, 72 h
Other metal-based compounds in comparison to cisplatin							
[36]	• Cu(II)- Casiopeina Igly • Cisplatin	 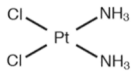	Human breast cancer MDA-MB-231 cells	^{1}H NMR	Cell extracts (acetonitrile/water)	IC_{50} at 24 h	20 min and 40 min
[37]	• Pd(II)Spermine • Cisplatin	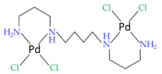 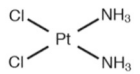	• Human osteosarcoma MG-63 cells • Human osteoblastic HOb cells	^{1}H HR-MAS	Cell lysates	IC_{50} at 24 h	12, 24, 36, 48, 72 h

Table 1. *Cont.*

Ref	Compound(s)	Structure(s)	Cell Line(s)	Type of Experiments	Sample Type(s)	Drug Treatment (Concentration)	Exposure Time
[38]	• Pd(II)Spermine • Pt(II)Spermine • Cisplatin • Oxaliplatin	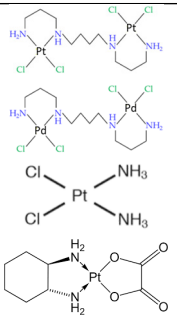	Human osteosarcoma MG-63 cells	^{1}H NMR	Cell extracts (m/c/w)	IC_{50} at 24 h	24, 48, 72 h
[39]	• Pd(II)Spermine • Pt(II)Spermine • Cisplatin • Oxaliplatin	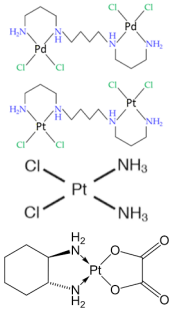	Human osteosarcoma MG-63 cells	^{1}H NMR	Lipidic extracts (m/c/w)	IC_{50} at 24 h	48 h
[40]	• Pd(II)Spermine • Cisplatin	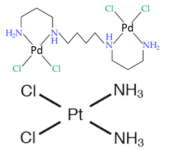	Breast cancer MDA-MB-231 cell-derived xenograft mouse model	^{1}H NMR	Cell extracts (m/c/w)	• Spermine: 5 mg/kg/day • Cisplatin: 2 mg/kg/day	5 days post-injection
[41]	• Pd(II)Spermine • Cisplatin	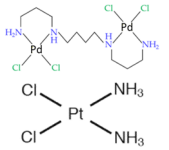	Six-week-old female BALB/cByJ mice	^{1}H NMR	Brain tissue extracts (m/c/w)	• Spermine: 3 mg/kg • Cisplatin: 3.5 mg/kg	1, 12, 48 h post-injection

The analysis of the endo-metabolome via cell lysates can be nicely complemented by the analysis of the exo-metabolome, i.e., the pool of metabolites presents in the extracellular medium. As the exo-metabolome is the result of an interchange of metabolites between cells and the culture medium, two groups of molecules can be identified, i.e., the taken-up substrates and the released metabolic products. The identification of the two groups of molecules can be easily achieved by the comparison of the cellular exo-metabolome with the profile of the "blank" growth medium.

The collection and analysis of the exo-metabolome samples is technically simple because it only requires centrifugation to separate culture media and cells [3].

Figure 3 reports the exo-metabolome of the A2780 ovarian cancer cell line growth in standard RPMI160 medium, GL261 glioblastoma cell line growth in DMEM medium, and DAOY medulloblastoma cell line growth in MEM medium.

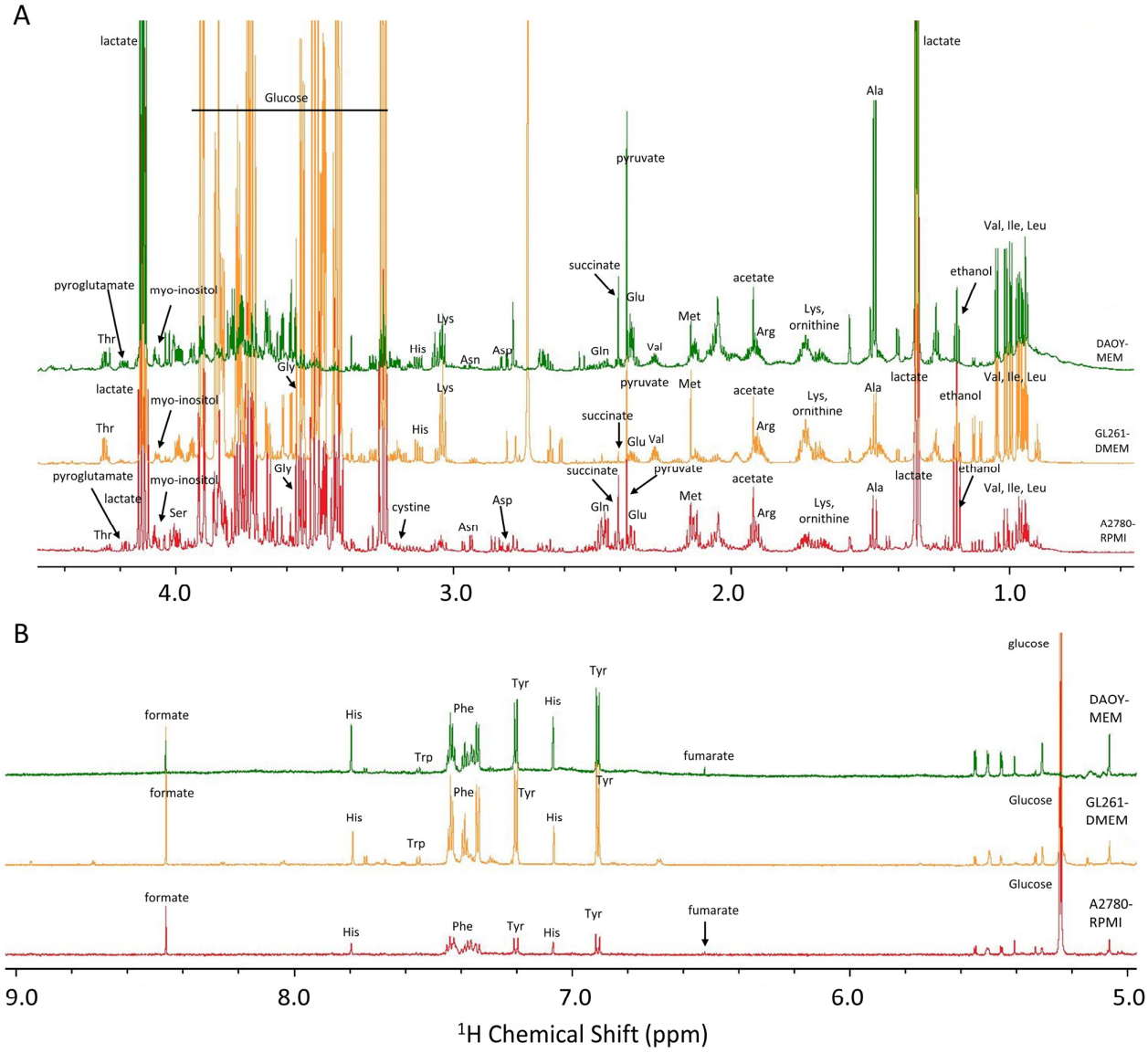

Figure 3. Representative ^{1}H NMR spectra of the exo-metabolome (growth media) of A2780 ovarian cancer cells (red trace), GL261 glioblastoma cells (yellow trace), and DAOY medulloblastoma cells (green trace). (**A**) Upfield (1.00–4.50 ppm) and (**B**) downfield (5.00–9.00 ppm) regions. The most abundant metabolites that have been identified in the spectra are indicated; for a graphical reason, for each metabolite only one (or more for a few cases) resonance is reported. The samples have been prepared according to the protocol reported in [3].

Highly complementary information can be obtained by a separate analysis of both the exo- and the endo-metabolome, and their integrated analysis provides a very accurate picture of the cell's metabolic behavior. Figure 4 reports the complete list of detected metabolites, in both cell lysates and growth media of A2780 cell line and their classification based on their chemical structures.

A

Metabolite	HMDB	PubChem	KEGG	Lysates	Growth media
3-hydroxyisovalerate	HMDB0000754	69362	C20827		X
3-methyl-2-oxovalerate	HMDB0000491	439286	C00671		X
4-hydoxyproline	HMDB0000725	5810	C01157	X	
acetate	HMDB0000042	176	C00033	X	X
acetone	HMDB0001659	180	C00207		X
L-alanine	HMDB0000161	5950	C00041	X	X
L-arginine	HMDB0000517	6322	C00062		X
L-asparagine	HMDB0000168	6267	C00152	X	X
L-aspartate	HMDB0000191	5960	C00049		X
AMP	HMDB0000045	6083	C00020	X	
ADP	HMDB0001341	6022	C00008	X	
ATP	HMDB0000538	5957	C00002	X	
choline	HMDB0000097	305	C00114	X	X
citrate	HMDB0000094	311	C00158	X	X
creatine	HMDB0000064	586	C00300	X	
L-cystine	HMDB0000192	67678	C00491		X
formate	HMDB0000142	284	C00058		X
fumarate	HMDB0000134	444972	C00122	X	X
D-glucose	HMDB0000122	5793	C00031		X
glucose-1-phosphate	HMDB0001586	65533	C00103	X	
glutamate	HMDB0000148	33032	C00025	X	X
glutamine	HMDB0000641	5961	C00064	X	X
glutathione	HMDB0000125	124886	C00051	X	
GPC	HMDB0000086	657272	C00670	X	
glycine	HMDB0000123	750	C00037	X	X
GTP	HMDB0001273	6830	C00044	X	
GDP	HMDB0001201	8977	C00035	X	
L-histidine	HMDB0000177	6274	C00135	X	X
IMP	HMDB0000175	8582	C00130	X	
L-isoleucine	HMDB0000172	6306	C00407	X	X
lactate	HMDB0000190	107689	C00186	X	X
L-leucine	HMDB0000687	6106	C00123	X	X
L-lysine	HMDB0000182	5962	C00047		X
methionine	HMDB0000696	6137	C00073		X
myo-inositol	HMDB0000211	NA	C00137	X	X
niacinamide	HMDB0001406	936	C00153	X	
ornithine	HMDB0000214	6262	C00077		X
L-phenylalanine	HMDB0000159	6140	C00079	X	X
phosphocholine	HMDB0001565	1014	C00588	X	
L-proline	HMDB0000162	145742	C00148		X
pyroglutamate	HMDB0000267	7405	C01879		X
pyruvate	HMDB0000243	1060	C00022		X
L-serine	HMDB0000187	5951	C00065		X
succinate	HMDB0000254	1110	C00042	X	X
taurine	HMDB0000251	1123	C00245	X	
L-tyrosine	HMDB0000158	6057	C00082	X	X
UDP-N-AcGln	HMDB0000290	445675	C00043	X	
UDP-N-AcGal	HMDB0000304	1167	C00203	X	
L-valine	HMDB0000883	6287	C00183	X	X

B

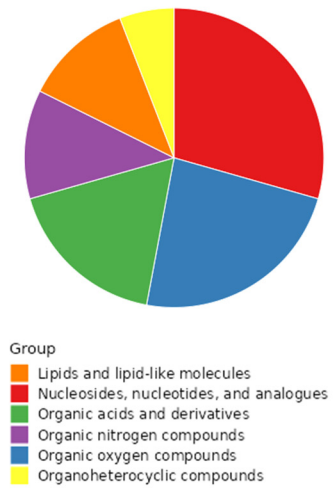

C

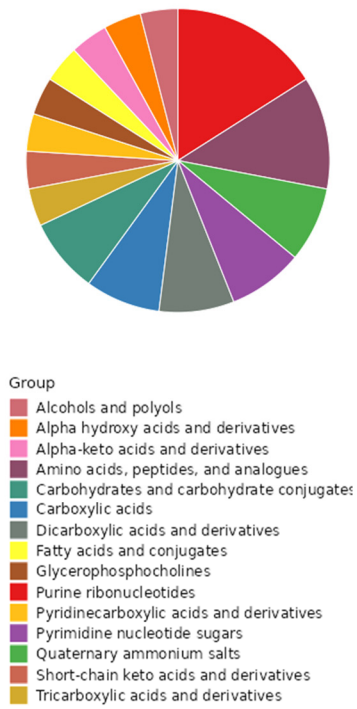

Figure 4. (**A**) List of detected metabolites in A2780 cells with KEGG and HMDB codes. (**B**,**C**) Enrichment analysis results: super (**B**) and sub-classes (**C**) classification according to their chemical structure, using the MetaboAnalyst 6.0 software [42].

Pathway analysis can be performed using the list of metabolites altered by treatment with drugs, with the final aim of obtaining a mechanistic explanation of the changes

observed, thus strengthening the information generated by the NMR analysis [43]. Different cell lines share the same main metabolic pathways (although with different weight of each of them on the overall metabolome), but the treatment with different compounds with different mechanisms of action will affect different biochemical processes. Online biological databases, such as KEGG (Kyoto Encyclopedia of Genes and Genomes) Pathway Database [44] or SMPD (Small Molecules Pathway Database) [45], provide information on a large number of metabolic pathways and can be easily consulted to identify and visualize how each metabolite is involved in the different biochemical pathways. Figure 5 reports the list of the metabolic pathways in which the metabolites identified in the NMR spectra of A2780 cells are involved.

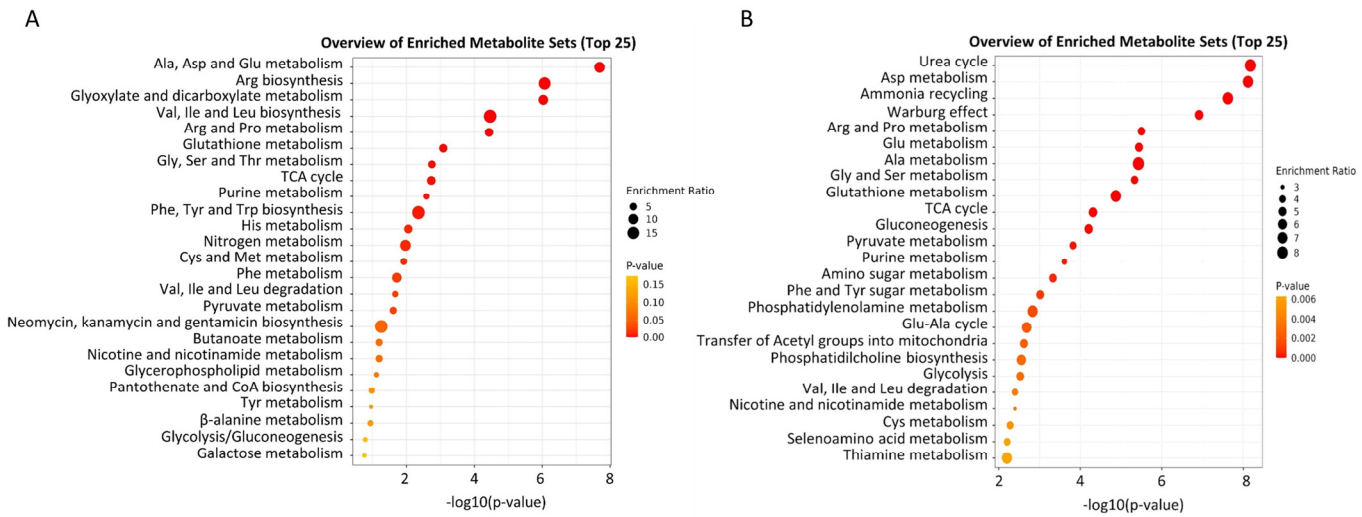

Figure 5. Enrichment analysis results: metabolic pathways with KEGG (**A**) and SMPD (**B**), using MetaboAnalyst 6.0 software [42].

In this framework, the selection of appropriate cell models to obtain biological pictures as similar as possible to the in vivo ones is of extreme importance. The comparison of the metabolomic profiles of patient-derived primary cells with those of established cell lines allows highlighting of the similarity and differences among the different cell types [15,46].

2. NMR Metabolomics and Metal-Based Compounds: State-of-the-Art

The study of the mechanisms of action of metallodrugs is fundamental for the development of more effective therapeutic strategies. As previously discussed, the detection of metabolic pathways altered upon treatment can be achieved by monitoring the changes over time. Table 1 reports the studies in the literature that have exploited NMR metabolomics to evaluate the metabolic responses of cancer cells to different metal-based drugs.

As expected, Pt(II)-based drugs are the most studied. The effects of cisplatin were characterized, alone or in comparison with other drugs (or drug candidates), in a variety of cancer cells by analyzing whole or lysed cells, respectively, via ^{1}H HR-MAS or using a solution of ^{1}H NMR for the analysis of cell lysates, extracts, and their cultured media. Despite the great variability of the observed cellular responses, mainly due to different cancer cell lines used and the largely different conditions of the various experiments, these studies revealed some common trends in the induced metabolic changes such as strong effects on lipid metabolism, membrane composition, a decrease in the overall cellular metabolic activities, and the alteration in the levels of some other diagnostic metabolites like the UDP-*N*-acetyl-glucosamine.

To our knowledge, only two metabolomic studies compared the metabolic effects induced by the three clinically approved Pt(II)-based drugs. The group of Ana Gill compared the effects of cisplatin and oxaliplatin in human osteosarcoma cells [39], while our research group compared the effects of cisplatin, carboplatin, and oxaliplatin in human

ovarian cancer cells [24]. Interestingly, the presence of different Pt(II)-based ligands in the square planar geometry of these molecules does not significantly affect the patterns of metabolomic alterations, but only seems to modulate the extent of the changes. In both cases, cisplatin produced the strongest effects.

The numerous side effects and the emergence of resistance to the clinically approved Pt(II)-based drugs have encouraged further development of platinum compounds as well as of other metal-based compounds as anticancer drug candidates. The cellular effects of two novel Pt(II)-based complexes were evaluated using ^{1}H NMR metabolomic profiling of cell extracts and cultured media. The [Pt(O,O′-acac)(γ-acac)(DMS)] complex showed very different metabolic changes with respect to cisplatin in the SKOV-3 cell line; in particular, higher levels of pyruvate were observed in addition to a very different lipid expression [29]. The mechanism of action of $[Pt(\eta^1\text{-}C_2H_4OMe)(DMSO)(phen)]^+$ was instead investigated on SH-SY5Y cells at different time points. The NMR data revealed a faster action of the new complex compared with cisplatin, with a response already observed after six hours of exposure, suggesting a cytosolic target with peculiar alteration of the glutathione metabolism pathway and of the diacylglycerol expression [30].

Due to the high similarity between Pt(II) and Pd(II), palladium chelates are among the molecules that have drawn increasing interest. In particular, the cellular effects of Pd(II)–spermine and Pt(II)–spermine complexes have been extensively characterized via ^{1}H NMR metabolomics in osteosarcoma cells, also in comparison to cisplatin and oxaliplatin [37–39,41]. In this case, it is the different metal center that modulates the extent of the typical changes in the cell metabolome. Treatment with Pd(II)–spermine showed weaker changes at the level of the metabolites but higher capability to modulate lipids and membrane compositions, in comparison to its Pt analogue.

To our knowledge, no NMR metabolomics studies were published on the cellular effects of the Ru-compounds that have been entered into the clinical trials (such as NAMI-A and NKP1339). Julier Furrer and collaborators tested two novel Ru-complexes (i.e., $(p\text{-cymene})_6Ru_6(tpt)_2(dhnq)_3]^{6+}$ and DiRu-1) on both cisplatin-sensitive and -resistant A2780 ovarian cancer cells and on human embryotic kidney HEK-293 cells via HR-MAS NMR analysis. While different metabolic responses were detected depending on the cell type and incubation time for $(p\text{-cymene})_6Ru_6(tpt)_2(dhnq)_3]^{6+}$ prims [17], the DiRu-1 complex showed an overall action on the redox homeostasis, the Warburg effect, and on lipid metabolism [34]. The third and latter tested Ru-compound via NMR metabolomics is GA113. The complex was tested for its anti-cancerous potential against a human malignant melanoma A375 cell line showing a high cytotoxicity. The six metabolites that were found to be altered after treatment are involved in (i) alanine, aspartate, and glutamate metabolic pathway, and (ii) glycine, serine, and threonine pathway [35].

Gold-based compounds represent another very interesting class of promising anticancer compounds [47]. Unlike Pt(II) compounds, gold(I) complexes have very low affinity for DNA, but they have very high affinity for cellular proteins with solvent-exposed cysteines or selenocysteines. Thus, due to the intrinsic nature of these metal centers, these molecules are supposed to give rise to multiple intracellular interactions with many functional proteins, rather than with a single enzyme or protein. In this context, our research group is carrying out a comparative NMR metabolomic study to analyze the responses of A2780 human ovarian cancer cells to a panel of selected gold(I) compounds, previously characterized with good anticancer properties. The obtained results for auranofin [31] and two carbene molecules [33] were published in 2020 and 2023, respectively. Interestingly, the treatment with the three compounds affects the metabolome of A2780 cells in different ways. Thus, contrary to what was observed for Pt(II)-based drugs, in this case it is the nature of the different gold(I) ligands that can modulate the reactivity of the compounds and also their intracellular targets resulting in substantially different modes of actions. For auranofin, both when administered alone [31] or conjugated with ferritin (to improve its targeted delivery towards cancer cells) [32], the most striking intracellular alteration was a very large and early increase of glutathione. The gold monocarbene and dicarbene

complexes behave differently from auranofin but display many alterations in common between the two of them; however, the latter amplifies the effects. Glycolysis is significantly affected and both drugs also caused a reduced uptake of several amino acids [33].

NMR metabolomics can also be applied in the study of drug treatment resistance. Again, almost all the examples present in the literature deal with cisplatin resistance. These works compared the metabolic profiles of the parental cisplatin-sensitive (i) ovarian cancer A2780 [15,24], (ii) breast cancer MDA-MB-231 [48], and (iii) lung adenocarcinoma A24 cell lines [49] with those of the respective derived cisplatin-resistant lines. The paired sensitive and resistant cell lines show significantly different profiles in terms of the concentrations of many metabolites, suggesting that the acquired cisplatin resistance is associated with multiple metabolic alterations. Interestingly, the different resistant cell lines share common changes for taurine, creatine, glutathione, myo-inositol and choline-containing compounds that can be considered putative markers of resistance insurgence. The relationship between the changes in membrane lipids and the cisplatin-resistance has also been studied via ^{1}H and ^{31}P NMR metabolomics in lung adenocarcinoma A549 cells [50]. The results indicated that components and properties of membrane phospholipids of cisplatin-sensitive and -resistant A549 cells (both before and after cisplatin treatment) were significantly different, highlighting the strong correlation between the biophysical properties of the cellular membranes and the development of resistance.

3. Conclusions

In this review, the application of NMR-based metabolomics of cell culture in metal-based drug research have been described.

NMR metabolomics can significantly contribute to the study of the mechanisms of action of drugs as it is an excellent investigative tool to characterize treatment-induced metabolic alterations at the cellular level according to an untargeted approach. This type of approach results are particularly suitable in the case of metallodrugs, which possess multiple and often unidentified intracellular targets.

^{1}H NMR spectral acquisition is relatively fast. Each cell lysate spectrum requires 30–60 min on average depending on the quantity of cells; only 5–15 minutes are instead required for the analysis of growth media. This permits to test multiple treatment conditions. In particular, studying different treatment times can allow us to detect both early and late cellular drug-induced events. Nevertheless, the reliability and reproducibility of the obtained results strongly depends upon the use of established procedures that avoid undesired changes in the metabolome induced by post-culture procedures.

Funding: This work has received funding from the Italian Ministry of Education and Research (MUR), through Department di Eccellenza 2023–2027 (DICUS 2.0) to the Department of Chemistry "Ugo Schiff" of the University of Florence.

Acknowledgments: The author acknowledges the support and the use of resources of Instruct-ERIC, a Landmark ESFRI project, and specifically the CERM/CIRMMP Italy Centre.

Conflicts of Interest: The authors declare no conflict of interest.

References

1. Mjos, K.D.; Orvig, C. Metallodrugs in Medicinal Inorganic Chemistry. *Chem. Rev.* **2014**, *114*, 4540–4563. [CrossRef] [PubMed]
2. Hanif, M.; Hartinger, C.G. Anticancer Metallodrugs: Where Is the next Cisplatin? *Future Med. Chem.* **2018**, *10*, 615–617. [CrossRef] [PubMed]
3. Ghini, V.; Meoni, G.; Vignoli, A.; Di Cesare, F.; Tenori, L.; Turano, P.; Luchinat, C. Fingerprinting and Profiling in Metabolomics of Biosamples. *Prog. Nucl. Magn. Reson. Spectrosc.* **2023**, *138–139*, 105–135. [CrossRef] [PubMed]
4. De Castro, F.; Benedetti, M.; Del Coco, L.; Fanizzi, F.P. NMR-Based Metabolomics in Metal-Based Drug Research. *Molecules* **2019**, *24*, 2240. [CrossRef] [PubMed]
5. Wishart, D.S.; Feunang, Y.D.; Marcu, A.; Guo, A.C.; Liang, K.; Vázquez-Fresno, R.; Sajed, T.; Johnson, D.; Li, C.; Karu, N.; et al. HMDB 4.0: The Human Metabolome Database for 2018. *Nucleic Acids Res.* **2018**, *46*, D608–D617. [CrossRef] [PubMed]
6. Cuperlović-Culf, M.; Barnett, D.A.; Culf, A.S.; Chute, I. Cell Culture Metabolomics: Applications and Future Directions. *Drug. Discov. Today* **2010**, *15*, 610–621. [CrossRef] [PubMed]

7. Eraslan, Z.; Cascante, M.; Günther, U.L. Metabolomics in Cell Biology. *Handb. Exp. Pharmacol.* **2023**, *277*, 181–207. [CrossRef] [PubMed]
8. Johnson, C.H.; Ivanisevic, J.; Siuzdak, G. Metabolomics: Beyond Biomarkers and towards Mechanisms. *Nat. Rev. Mol. Cell Biol.* **2016**, *17*, 451–459. [CrossRef] [PubMed]
9. Halama, A. Metabolomics in Cell Culture—A Strategy to Study Crucial Metabolic Pathways in Cancer Development and the Response to Treatment. *Arch. Biochem. Biophys.* **2014**, *564*, 100–109. [CrossRef]
10. Wang, Z.; Pisano, S.; Ghini, V.; Kadeřávek, P.; Zachrdla, M.; Pelupessy, P.; Kazmierczak, M.; Marquardsen, T.; Tyburn, J.-M.; Bouvignies, G.; et al. Detection of Metabolite-Protein Interactions in Complex Biological Samples by High-Resolution Relaxometry: Toward Interactomics by NMR. *J. Am. Chem. Soc.* **2021**, *143*, 9393–9404. [CrossRef]
11. Barrilero, R.; Ramírez, N.; Vallvé, J.C.; Taverner, D.; Fuertes, R.; Amigó, N.; Correig, X. Unravelling and Quantifying the "NMR-Invisible" Metabolites Interacting with Human Serum Albumin by Binding Competition and T2 Relaxation-Based Decomposition Analysis. *J. Proteome Res.* **2017**, *16*, 1847–1856. [CrossRef] [PubMed]
12. Bhinderwala, F.; Evans, P.; Jones, K.; Laws, B.R.; Smith, T.G.; Morton, M.; Powers, R. Phosphorus NMR and Its Application to Metabolomics. *Anal. Chem.* **2020**, *92*, 9536–9545. [CrossRef] [PubMed]
13. Filippov, A.V.; Khakimov, A.M.; Munavirov, B.V. Chapter Two—31P NMR Studies of Phospholipids. In *Annual Reports on NMR Spectroscopy*; Webb, G.A., Ed.; Academic Press: Cambridge, MA, USA, 2015; Volume 85, pp. 27–92.
14. Kostidis, S.; Addie, R.D.; Morreau, H.; Mayboroda, O.A.; Giera, M. Quantitative NMR Analysis of Intra- and Extracellular Metabolism of Mammalian Cells: A Tutorial. *Anal. Chim. Acta* **2017**, *980*, 1–24. [CrossRef]
15. Ghini, V.; Sorbi, F.; Fambrini, M.; Magherini, F. NMR Metabolomics of Primary Ovarian Cancer Cells in Comparison to Established Cisplatin-Resistant and -Sensitive Cell Lines. *Cells* **2024**, *13*, 661. [CrossRef] [PubMed]
16. Moestue, S.; Sitter, B.; Bathen, T.F.; Tessem, M.-B.; Gribbestad, I.S. HR MAS MR Spectroscopy in Metabolic Characterization of Cancer. *Curr. Top. Med. Chem.* **2011**, *11*, 2–26. [CrossRef] [PubMed]
17. Vermathen, M.; Paul, L.E.H.; Diserens, G.; Vermathen, P.; Furrer, J. 1H HR-MAS NMR Based Metabolic Profiling of Cells in Response to Treatment with a Hexacationic Ruthenium Metallaprism as Potential Anticancer Drug. *PLoS ONE* **2015**, *10*, e0128478. [CrossRef] [PubMed]
18. Diserens, G.; Vermathen, M.; Zurich, M.-G.; Vermathen, P. Longitudinal Investigation of the Metabolome of 3D Aggregating Brain Cell Cultures at Different Maturation Stages by 1H HR-MAS NMR. *Anal. Bioanal. Chem.* **2018**, *410*, 6733–6749. [CrossRef] [PubMed]
19. Liu, S.; Wang, W.; Zhou, X.; Gu, R.; Ding, Z. Dose Responsive Effects of Cisplatin in L02 Cells Using NMR-Based Metabolomics. *Env. Toxicol. Pharmacol.* **2014**, *37*, 150–157. [CrossRef] [PubMed]
20. Duarte, I.F.; Ladeirinha, A.F.; Lamego, I.; Gil, A.M.; Carvalho, L.; Carreira, I.M.; Melo, J.B. Potential Markers of Cisplatin Treatment Response Unveiled by NMR Metabolomics of Human Lung Cells. *Mol. Pharm.* **2013**, *10*, 4242–4251. [CrossRef]
21. Pan, X.; Wilson, M.; McConville, C.; Arvanitis, T.N.; Griffin, J.L.; Kauppinen, R.A.; Peet, A.C. Increased Unsaturation of Lipids in Cytoplasmic Lipid Droplets in DAOY Cancer Cells in Response to Cisplatin Treatment. *Metabolomics* **2013**, *9*, 722–729. [CrossRef]
22. Duarte, I.F.; Lamego, I.; Marques, J.; Marques, M.P.M.; Blaise, B.J.; Gil, A.M. Nuclear Magnetic Resonance (NMR) Study of the Effect of Cisplatin on the Metabolic Profile of MG-63 Osteosarcoma Cells. *J. Proteome Res.* **2010**, *9*, 5877–5886. [CrossRef] [PubMed]
23. Pan, X.; Wilson, M.; Mirbahai, L.; McConville, C.; Arvanitis, T.N.; Griffin, J.L.; Kauppinen, R.A.; Peet, A.C. In Vitro Metabonomic Study Detects Increases in UDP-GlcNAc and UDP-GalNAc, as Early Phase Markers of Cisplatin Treatment Response in Brain Tumor Cells. *J. Proteome Res.* **2011**, *10*, 3493–3500. [CrossRef] [PubMed]
24. Ghini, V.; Magherini, F.; Massai, L.; Messori, L.; Turano, P. Comparative NMR Metabolomics of the Responses of A2780 Human Ovarian Cancer Cells to Clinically Established Pt-Based Drugs. *Dalton Trans.* **2022**, *51*, 12512–12523. [CrossRef] [PubMed]
25. Del Coco, L.; Majellaro, M.; Boccarelli, A.; Cellamare, S.; Altomare, C.D.; Fanizzi, F.P. Novel Antiproliferative Biphenyl Nicotinamide: NMR Metabolomic Study of Its Effect on the MCF-7 Cell in Comparison with Cisplatin and Vinblastine. *Molecules* **2020**, *25*, 3502. [CrossRef] [PubMed]
26. Lamego, I.; Duarte, I.F.; Marques, M.P.M.; Gil, A.M. Metabolic Markers of MG-63 Osteosarcoma Cell Line Response to Doxorubicin and Methotrexate Treatment: Comparison to Cisplatin. *J. Proteome Res.* **2014**, *13*, 6033–6045. [CrossRef] [PubMed]
27. Maria, R.M.; Altei, W.F.; Selistre-de-Araujo, H.S.; Colnago, L.A. Impact of Chemotherapy on Metabolic Reprogramming: Characterization of the Metabolic Profile of Breast Cancer MDA-MB-231 Cells Using 1H HR-MAS NMR Spectroscopy. *J. Pharm. Biomed Anal.* **2017**, *146*, 324–328. [CrossRef] [PubMed]
28. Lin, C.; Dong, J.; Wei, Z.; Cheng, K.-K.; Li, J.; You, S.; Liu, Y.; Wang, X.; Chen, Z. 1H NMR-Based Metabolic Profiles Delineate the Anticancer Effect of Vitamin C and Oxaliplatin on Hepatocellular Carcinoma Cells. *J. Proteome Res.* **2020**, *19*, 781–793. [CrossRef]
29. De Castro, F.; Benedetti, M.; Antonaci, G.; Del Coco, L.; De Pascali, S.A.; Muscella, A.; Marsigliante, S.; Fanizzi, F.P. Response of Cisplatin Resistant Skov-3 Cells to [Pt(O,O′-Acac)(γ-Acac)(DMS)] Treatment Revealed by a Metabolomic ^{1}H-NMR Study. *Molecules* **2018**, *23*, 2301. [CrossRef]
30. De Castro, F.; Stefàno, E.; De Luca, E.; Muscella, A.; Marsigliante, S.; Benedetti, M.; Fanizzi, F.P. A NMR-Based Metabolomic Approach to Investigate the Antitumor Effects of the Novel [Pt(η 1-C2H4OMe)(DMSO)(Phen)]+ (Phen = 1,10-Phenanthroline) Compound on Neuroblastoma Cancer Cells. *Bioinorg. Chem. Appl.* **2022**, *2022*, 8932137. [CrossRef]
31. Ghini, V.; Senzacqua, T.; Massai, L.; Gamberi, T.; Messori, L.; Turano, P. NMR Reveals the Metabolic Changes Induced by Auranofin in A2780 Cancer Cells: Evidence for Glutathione Dysregulation. *Dalton Trans.* **2021**, *50*, 6349–6355. [CrossRef]

32. Cosottini, L.; Massai, L.; Ghini, V.; Zineddu, S.; Geri, A.; Mannelli, M.; Ciambellotti, S.; Severi, M.; Gamberi, T.; Messori, L.; et al. Bioconjugation of the Gold Drug Auranofin to Human Ferritin Yields a Potent Cytotoxin. *J. Drug Deliv. Sci. Technol.* **2023**, *87*, 104822. [CrossRef]
33. Ghini, V.; Mannelli, M.; Massai, L.; Geri, A.; Zineddu, S.; Gamberi, T.; Messori, L.; Turano, P. The Effects of Two Cytotoxic Gold(i) Carbene Compounds on the Metabolism of A2780 Ovarian Cancer Cells: Mechanistic Inferences through NMR Analysis. *RSC Adv.* **2023**, *13*, 21629–21632. [CrossRef] [PubMed]
34. Primasová, H.; Paul, L.E.H.; Diserens, G.; Primasová, E.; Vermathen, P.; Vermathen, M.; Furrer, J. 1H HR-MAS NMR-Based Metabolomics of Cancer Cells in Response to Treatment with the Diruthenium Trithiolato Complex [(p-MeC6H4iPr)2Ru2(SC6H4-p-But)3]+ (DiRu-1). *Metabolites* **2019**, *9*, 146. [CrossRef] [PubMed]
35. Hussan, A.; Moyo, B.; Amenuvor, G.; Meyer, D.; Sitole, L. Investigating the Antitumor Effects of a Novel Ruthenium (II) Complex on Malignant Melanoma Cells: An NMR-Based Metabolomic Approach. *Biochem. Biophys. Res. Commun.* **2023**, *686*, 149169. [CrossRef] [PubMed]
36. Resendiz-Acevedo, K.; García-Aguilera, M.E.; Esturau-Escofet, N.; Ruiz-Azuara, L. 1H -NMR Metabolomics Study of the Effect of Cisplatin and Casiopeina IIgly on MDA-MB-231 Breast Tumor Cells. *Front. Mol. Biosci.* **2021**, *8*, 1135. [CrossRef]
37. Lamego, I.; Marques, M.P.M.; Duarte, I.F.; Martins, A.S.; Oliveira, H.; Gil, A.M. Impact of the Pd2Spermine Chelate on Osteosarcoma Metabolism: An NMR Metabolomics Study. *J. Proteome Res.* **2017**, *16*, 1773–1783. [CrossRef]
38. Martins, A.S.; Batista de Carvalho, A.L.M.; Marques, M.P.M.; Gil, A.M. Response of Osteosarcoma Cell Metabolism to Platinum and Palladium Chelates as Potential New Drugs. *Molecules* **2021**, *26*, 4805. [CrossRef]
39. Bispo, D.S.C.; Correia, M.; Carneiro, T.J.; Martins, A.S.; Reis, A.A.N.; de Carvalho, A.L.M.B.; Marques, M.P.M.; Gil, A.M. Impact of Conventional and Potential New Metal-Based Drugs on Lipid Metabolism in Osteosarcoma MG-63 Cells. *Int. J. Mol. Sci.* **2023**, *24*, 17556. [CrossRef] [PubMed]
40. Carneiro, T.J.; Araújo, R.; Vojtek, M.; Gonçalves-Monteiro, S.; de Carvalho, A.L.M.B.; Marques, M.P.M.; Diniz, C.; Gil, A.M. Impact of the Pd2Spm (Spermine) Complex on the Metabolism of Triple-Negative Breast Cancer Tumors of a Xenograft Mouse Model. *Int. J. Mol. Sci.* **2021**, *22*, 10775. [CrossRef]
41. Carneiro, T.J.; Vojtek, M.; Gonçalves-Monteiro, S.; Neves, J.R.; de Carvalho, A.L.M.B.; Marques, M.P.M.; Diniz, C.; Gil, A.M. Metabolic Impact of Anticancer Drugs Pd2Spermine and Cisplatin on the Brain of Healthy Mice. *Pharmaceutics* **2022**, *14*, 259. [CrossRef]
42. Chong, J.; Soufan, O.; Li, C.; Caraus, I.; Li, S.; Bourque, G.; Wishart, D.S.; Xia, J. MetaboAnalyst 4.0: Towards More Transparent and Integrative Metabolomics Analysis. *Nucleic. Acids Res.* **2018**, *46*, W486–W494. [CrossRef] [PubMed]
43. Tsouka, S.; Masoodi, M. Metabolic Pathway Analysis: Advantages and Pitfalls for the Functional Interpretation of Metabolomics and Lipidomics Data. *Biomolecules* **2023**, *13*, 244. [CrossRef]
44. Kanehisa, M.; Goto, S. KEGG: Kyoto Encyclopedia of Genes and Genomes. *Nucleic Acids Res.* **2000**, *28*, 27–30. [CrossRef] [PubMed]
45. Jewison, T.; Su, Y.; Disfany, F.M.; Liang, Y.; Knox, C.; Maciejewski, A.; Poelzer, J.; Huynh, J.; Zhou, Y.; Arndt, D.; et al. SMPDB 2.0: Big Improvements to the Small Molecule Pathway Database. *Nucleic Acids Res.* **2014**, *42*, D478–D484. [CrossRef] [PubMed]
46. Ramachandran, G.K.; Yeow, C.H. Proton NMR Characterization of Intact Primary and Metastatic Melanoma Cells in 2D & 3D Cultures. *Biol. Res.* **2017**, *50*, 12. [CrossRef] [PubMed]
47. Nobili, S.; Mini, E.; Landini, I.; Gabbiani, C.; Casini, A.; Messori, L. Gold Compounds as Anticancer Agents: Chemistry, Cellular Pharmacology, and Preclinical Studies. *Med. Res. Rev.* **2010**, *30*, 550–580. [CrossRef]
48. Carneiro, T.J.; Carvalho, A.L.M.B.; Vojtek, M.; Carmo, I.F.; Marques, M.P.M.; Diniz, C.; Gil, A.M. Disclosing a Metabolic Signature of Cisplatin Resistance in MDA-MB-231 Triple-Negative Breast Cancer Cells by NMR Metabolomics. *Cancer Cell Int.* **2023**, *23*, 310. [CrossRef] [PubMed]
49. Vermathen, M.; von Tengg-Kobligk, H.; Hungerbühler, M.N.; Vermathen, P.; Ruprecht, N. 1H HR-MAS NMR Based Metabolic Profiling of Lung Cancer Cells with Induced and De-Induced Cisplatin Resistance to Reveal Metabolic Resistance Adaptations. *Molecules* **2021**, *26*, 6766. [CrossRef]
50. Huang, Z.; Tong, Y.; Wang, J.; Huang, Y. NMR Studies of the Relationship between the Changes of Membrane Lipids and the Cisplatin-Resistance of A549/DDP Cells. *Cancer Cell Int.* **2003**, *3*, 5. [CrossRef]